Published in Dalton Transactions 40, issue 27, 7172-7180, 2011
which should be used for any reference to this work

Anticancer activity of tetracationic arene ruthenium metalla-cycles

Nicolas P. E. Barry,[a] Fabio Edafe[b] and Bruno Therrien*[a]

[a]*Institute of Chemistry, University of Neuchatel, 51 Ave de Bellevaux, CH- 2000 Neuchatel, Switzerland. E-mail: bruno.therrien@unine.ch; Fax: +41 32 7182511*
[b]*Institut des Sciences et Ingénierie Chimique, Ecole Polytechnique Fédérale de Lausanne (EPFL), CH-1015 Lausanne, Switzerland*

A series of cationic metalla-cycles of the general formulae $[(\eta^6\text{-}p\text{-cym})_4Ru_4(OO\cap OO)_2(N\cap N)_2]^{4+}$ and $[(\eta^6\text{-}p\text{-cym})_4Ru_4(NO\cap NO)_2(N\cap N)_2]^{4+}$ has been prepared from the dinuclear arene ruthenium precursors $[(\eta^6\text{-}p\text{-cym})_2Ru_2(OO\cap OO)_2Cl_2]$ ($OO\cap OO$ = oxalato, 1,4-benzoquinonato-2,5-diolato, 1,4-naphtoquinonato-5,8-diolato, 9,10-anthraquinonato-1,4-diolato, 5,12-tetraquinonato-6,11-diolato) and $[(\eta^6\text{-}p\text{-cym})_2Ru_2(NO\cap NO)_2Cl_2]$ ($NO\cap NO$ = oxamido, oxonico) by reaction with two different bidentate linkers ($N\cap N$ = 1,2-bis(4-pyridyl)ethylene, 1,2-bis(4-pyridyl)ethane) in the presence of silver triflate. All complexes were isolated as triflate salts and characterised by NMR, infrared, UV-visible, mass spectrometry and by elemental analysis. The cytotoxicities of the tetranuclear ruthenium complexes have been established using ovarian A2780 and A2780cisR cancer cell lines. All complexes exhibit moderate to excellent activity on both the cisplatin resistant and cisplatin sensitive cells, thus suggesting a mode of action different from cisplatin.

Introduction

The design of molecular hosts to encapsulate guest molecules in a confined environment is receiving considerable attention due to the analogy of these systems with the mode of action of enzymes. Pioneered by Cram, Lehn and Pedersen,[1] winners of the Nobel Prize in chemistry in 1987 for their contributions to the development and use of molecules with structure-specific interactions of high selectivity, synthetic molecular hosts were initially dominated by purely organic molecules: cyclodextrins, carcerands, cryptands, cucurbiturils, cavitands.[2] However, the last twenty years have seen the emergence of discrete inorganic and organometallic metalla-hosts able to encapsulate temporary or permanently various guest molecules in their cavity, thus opening new perspectives in coordination chemistry.[3] In analogy to crown-ethers, 15 years ago, Fish and his co-workers have prepared a series of trinuclear metalla-cycles composed of half-sandwich complexes and adenine-derivative ligands.[4] Molecular modelling suggested classical π–π interactions between the aromatic groups of various substituted aromatic carboxylic acids and the cavity of the trinuclear hosts. Using a similar strategy, other trinuclear metalla-cycles have been isolated,[5] and nowadays, tetranuclear[6] as well as hexanuclear metalla-cycles[7] composed of half-sandwich complexes can be found in the literature. For example, trinuclear metalla-cycles derived from half-sandwich complexes and 2,3-dihydroxypyridine ligands have been found to possess high affinity for lithium and sodium salts, thus giving rise to potential sensors.[8] Moreover, it was found that tetranuclear arene ruthenium metalla-cycles interact strongly with DNA[9] and are cytotoxic on various cancer cell lines.[10] Similarly, cationic tetranuclear arene osmium metalla-cycles have shown cytotoxicity on human ovarian cancer cells.[11] These examples confirm the potential of using metalla-cycles composed of half-sandwich complexes to prepare biological agents. Among these half-sandwich complexes for biological applications, arene ruthenium complexes are probably the derivatives receiving the greatest attention.[12]

Since 2008, we are exploiting the combination of supramolecular chemistry of half-sandwich building blocks with the antitumoral and antimetastatic activity of arene ruthenium complexes.[13] It has been demonstrated that water-soluble arene ruthenium metalla-assemblies are stable in biological medium, exhibit antiproliferative activity, and they can act as drug carriers. This approach has led to the synthesis of tetranuclear metalla-cycles,[14] hexanuclear metalla-prisms,[15] as well as octanuclear metalla-boxes.[16] In particular, tetranuclear arene ruthenium metalla-cycles of the general formula $[(\eta^6\text{-arene})_4Ru_4(OO\cap OO)_2(N\cap N)_2]^{4+}$ (arene = *para*-cymene (*p*-cym), hexamethylbenzene (hmb); $OO\cap OO$ = 1,4-benzoquinonato-2,5-diolato (dobq), 3,6-dichlorido-1,4-benzoquinonato (dcbq); $N\cap N$ = pyrazine (pyr), 4,4′-bipyridine (bpy), 1,2-bis(4-pyridyl)ethylene (bpe)) have been tested against cancer cells. The activity of these metalla-cycles against human ovarian cancer cell lines (A2780 and A2780cisR) was found to be moderate to excellent, depending on the size of the linker used as well as the nature of the arene ligand (*p*-cym, hmb), with IC_{50} values as low as 4 μM.[17]

To further study the antiproliferative activity of arene ruthenium metalla-cycles, we propose to investigate the role played by the linkers as well as the role played by the

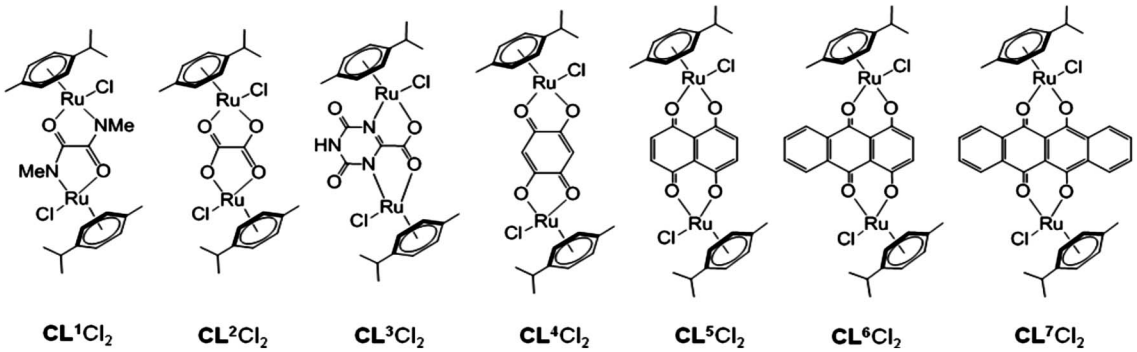

Chart 1

length and nature of the metalla-clips in the cytotoxicity of tetranuclear metalla-cycles. Herein, we describe the synthesis and the characterisation of 14 metalla-cycles of the general formulae $[(\eta^6\text{-}p\text{-cym})_4Ru_4(OO\cap OO)_2(N\cap N)_2]^{4+}$ and $[(\eta^6\text{-}p\text{-cym})_4Ru_4(NO\cap NO)_2(N\cap N)_2]^{4+}$ ($OO\cap OO$ = oxalato (ox), dobq, 1,4-naphtoquinonato-5,8-diolato (donq), 9,10-anthraquinonato-1,4-diolato (doaq), 5,12-tetraquinonato-6,11-diolato (dotq); $NO\cap NO$ = oxamido (oxa), oxonico (oxo); $N\cap N$ = bpe, 1,2-bis(4-pyridyl)ethane (bpa)), prepared from the dinuclear complexes **CL**^{1}Cl_2–**CL**^{7}Cl_2 (see Chart 1). In addition, the *in vitro* anticancer activity of these arene ruthenium metalla-cycles against human ovarian cancer cell lines (A2780 and A2780cisR) is reported and compared to cisplatin.

Results and discussion

Synthesis and characterisation

The synthesis of the arene ruthenium metalla-cycles incorporating 1,2-bis(4-pyridyl)ethylene (bpe) linkers, **2a**,[14b] **4a**,[17] **5a**,[15b] **6a**,[14a] and **7a**,[14a] is straightforward, as previously described in the literature. Accordingly, the preparation of the 1,2-bis(4-pyridyl)ethane (bpa) derivatives involves the addition of four equivalents of silver triflate to two equivalents of the dinuclear metalla-clips $[(\eta^6\text{-}p\text{-cym})_2Ru_2(OO\cap OO)_2Cl_2]$ ($OO\cap OO$ = ox, dobq, donq, doaq, dotq) (**CL**^{2}Cl_2 and **CL**^{4}Cl_2–**CL**^{7}Cl_2) in the presence of two equivalents of bpa. These tetracationic metalla-cycles (**2b**, **4b**, **5b**, **6b**, and **7b**) are isolated in good yield as triflate salts. All arene ruthenium metalla-cycles used in this study are presented in Fig. 1.

Following the same strategy in which the new dinuclear complex $[(\eta^6\text{-}p\text{-cym})_2Ru_2(oxa)_2Cl_2]$ (**CL**^{1}Cl_2) and the already known dinuclear complex $[(\eta^6\text{-}p\text{-cym})_2Ru_2(oxo)_2Cl_2]$[9] (**CL**^{3}$Cl_2$) are used as metalla-clips with bpe and bpa as $N\cap N$ linkers, the salts [**1a**:**1b**][CF_3SO_3]$_4$ and [**3a**:**3b**][CF_3SO_3]$_4$ have been prepared. These new metalla-cycles were isolated as triflate salts and fully characterised.

The solubility of all metalla-cycles is quite high in dichloromethane, acetonitrile, acetone and dimethyl sulfoxide but low in methanol and water. However, in the case of the bpa derivatives (**1b–7b**) a higher water-solubility is observed. The stability of all metalla-cycles is excellent in a mixture of D_2O and DMSO-d_6 (50 : 50; v : v) as monitored by ^{1}H NMR in which after 12 h of heating at 37 °C, no degradation was observed. Salts [**1a–7a**][CF_3SO_3]$_4$ and [**1b–7b**][CF_3SO_3]$_4$ have been characterised by IR, UV-visible, NMR spectroscopy, mass spectrometry and by elemental analysis.

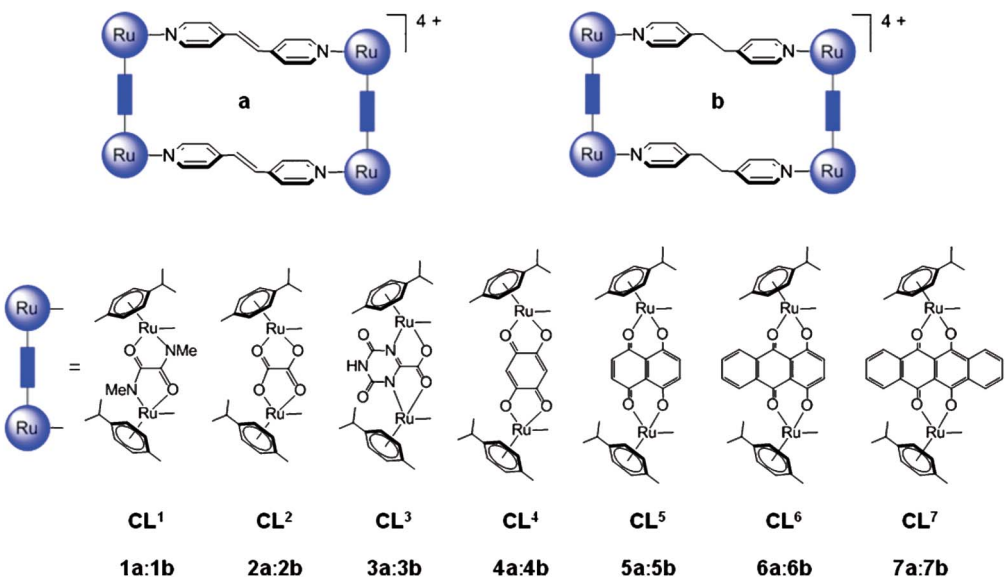

Fig. 1 Metalla-cycles **1a–7a** and **1b–7b**.

The infrared spectra of all the metalla-cycles are dominated by absorptions of the coordinated *N*∩*N*, *OO*∩*OO* and *NO*∩*NO* ligands, which are only slightly shifted as compared to the infrared absorptions of the free ligands. In all metalla-clips as well as in all metalla-cycles, a significant redshift of about 20 cm^{-1} is observed for the C═O vibration frequencies as compared to the frequencies of non-coordinated bridging ligands. This can be attributed to a decrease in the CO bond order upon coordination with ruthenium atoms.[18] This decrease of the CO bond order leading to a redshift of the CO absorption is consistent with the X-ray data of the dinuclear complex $[\mathbf{CL}^5(OH_2)_2]^{2+}$,[19] for which the lengths of the CO bonds are comprised between 1.27(1) Å and 1.32(2) Å, suggesting an intermediate bond order between single (~1.40 Å) and double (~1.20 Å).[20] Furthermore, in metalla-cycles **3a** and **3b** strong absorptions due to the stretching vibrations of C═N oxonico bridging ligands are observed at around 1710 cm^{-1} alongside the absorptions of the stretching vibrations of the C═O bridging ligands at around 1600 cm^{-1}. In addition to these CN and CO signals, strong absorptions due to the stretching vibrations of the triflate anions (1260(s), 1030(s), 638(m) cm^{-1}) are observed in the infrared spectra of all the salts **[1a–7a]**$[CF_3SO_3]_4$ and **[1b–7b]**$[CF_3SO_3]_4$.

The electronic absorption spectra of all metalla-cycles are characterised by an intense high-energy band centred at 270 nm, which is attributed to ligand π → π* transitions.[21] A broad, moderately intense absorption band in the visible region (see inset in Fig. 2) is tentatively assigned to mixed metal-to-ligand charge transfer (MLCT), intra-ligand charge transfer (ILCT) and ligand π → π* transitions, where ILCT refers to intra-ligand charge transfer from the bpe or bpa *N*∩*N* linkers to the *OO*∩*OO* or *NO*∩*NO* bridging ligands.[22] Moreover, in the metalla-cycles incorporating quinone derivatives (**4a–7a** and **4b–7b**) several bands attributed to ILCT are observed in the visible region between 500 and 800 nm. The UV-visible spectra in dichloromethane (10^{-5} M) of metalla-cycles **1b–7b** are presented in Fig. 2.

Moreover, bathochromic shifts are observed between the arene ruthenium metalla-cycles incorporating the 1,2-bis(4-pyridyl)ethylene linkers (**5a–7a**) and the metalla-cycles incorporating the 1,2-bis(4-pyridyl)ethane linkers (**5b–7b**). This significant bathochromic shift of up to 13 nm of λ_{max} in the case of **7a**:**7b** is presumably due to a lower contribution to intra-ligand charge transfer transitions (ILCT) from the bpa linkers to the *OO*∩*OO* bridging ligands as compared to the same ILCT from bpe linkers to the corresponding quinone bridging ligands.[23] The bathochromic shifts of absorption bands of metalla-cycles **5a**:**5b**, **6a**:**6b** and **7a**:**7b** between 550 and 800 nm are depicted in Fig. 3.

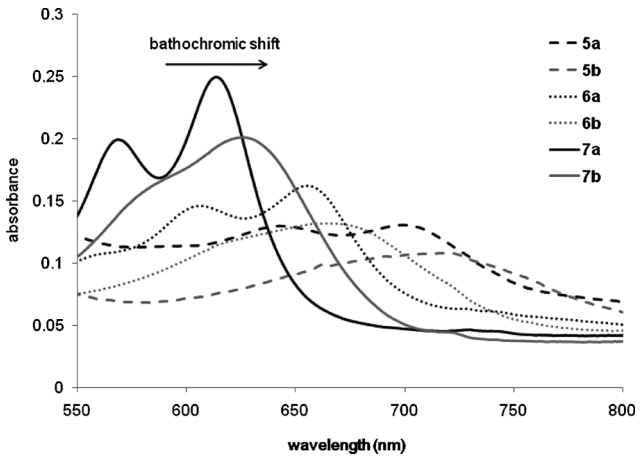

Fig. 3 Bathochromic effect observed in the UV-visible spectra of **5a**:**5b** (---), **6a**:**6b** (· · ·) and **7a**:**7b** (—) (CH_2Cl_2, 10^{-5} M).

The ^{1}H NMR spectra of **2b** and **4b–7b** display two doublets between 7.0 and 9.0 ppm due to the pyridyl protons of the bpa ligands. Unlike free bpa, where the signals of the pyridyl protons are found at $\delta = 8.54$ (H_α) and 7.21 ppm (H_β) respectively (CD_3CN, 21 °C), the signal of H_α in **2b** and **4b–7b** appears slightly to strongly upfield shifted (up to 0.80 ppm in the case of **2b**), while the signal of H_β is either shifted upfield (**2b**, **4b**, **5b**) or downfield (**6b** and **7b**). The same behaviour is observed for the metalla-cycles incorporating the bpe linkers, where a significant upfield shift of the H_α signal (up to 0.75 ppm) and either an upfield or downfield shift of the H_β signal are observed. Singlet associated

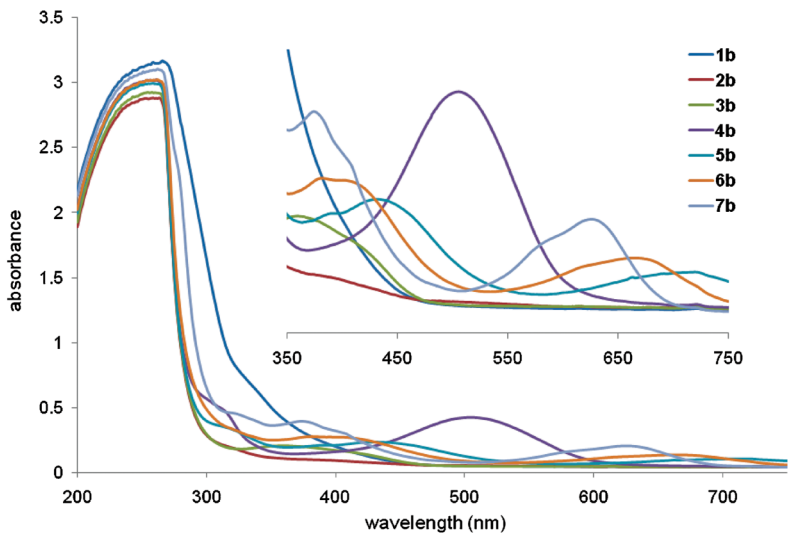

Fig. 2 UV-visible spectra of **[1b–7b]**$[CF_3SO_3]_4$ in CH_2Cl_2 (10^{-5} M).

of the ethane protons in compounds **1b–7b** (broad in the case of **3b**) is observed at around 3.30 ppm. This important upfield shift of about 0.40 ppm for this signal as compared to the chemical shift of the ethane signals in free bpa (2.92 ppm in CD_3CN, 21 °C) is characteristic of the formation of metalla-cycles.[24] Indeed, this observation is in accordance with the chemical displacement of the ethylene protons observed in complexes **1a–7a** where such an upfield shift (~0.30 ppm) is observed for the $H_{C=C}$ signals. Finally, the arene protons and the protons of the *OO*∩*OO* and *NO*∩*NO* bridging ligands are not strongly influenced by the cyclisation and show almost the same chemical shifts in both the metalla-cycles and the dinuclear metalla-clips (**CL**^{1}Cl_2–**CL**^{7}Cl_2).[14]

It is noteworthy that among the seven dinuclear arene ruthenium precursors, three are potentially chiral, **CL**^{1}Cl_2, **CL**^{3}Cl_2 and **CL**^{6}Cl_2 respectively. These dinuclear complexes possess the ability to form *racemic* and *meso* stereoisomers (Fig. 4), if the chlorido ligands are not sterically restricted to coordinate at particular positions. In addition, the two diastereoisomers can be observed by NMR spectroscopy only if the metal centres are configurationally stable in solution.[25] Nevertheless, upon formation of the corresponding tetranuclear metalla-cycles **1**, **3** and **6**, and despite the presence of four stereogenic ruthenium centres, only two diastereoisomers are observed. The two isomers observed in **1** are presented in Fig. 5.

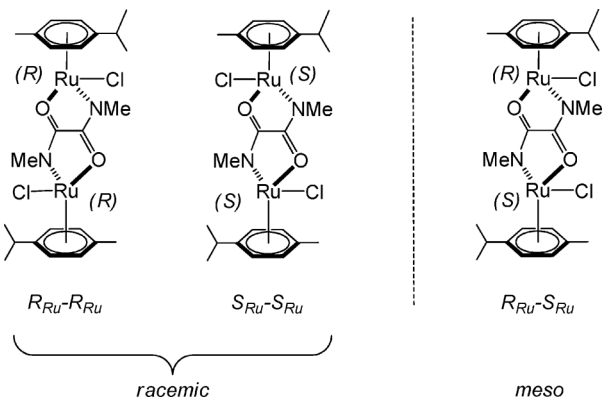

Fig. 4 *Racemic* and *meso* stereoisomers of metalla-clip **CL**^{1}Cl_2.

Indeed, in the ^{1}H NMR spectra of metalla-cycles **1a**:**1b** and **3a**:**3b** (see Fig. 6) the presence of these two isomers leads to two distinct sets of signals for the pyridyl protons H_α and H_β (CD_3CN, 21 °C). Furthermore in metalla-cycles **1a** and **3a** the two sets of signals are relatively broad and present almost similar chemical shifts, while in **1b** and **3b** the two sets are less broadened and more defined. This different behaviour between metalla-cycles

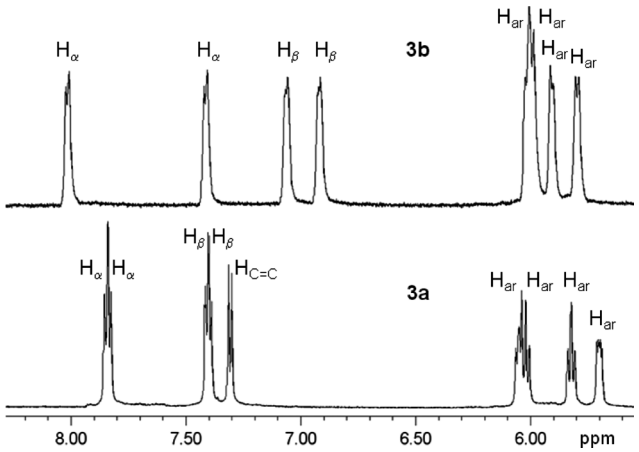

Fig. 6 ^{1}H NMR spectra in CD_3CN (21 °C) of metalla-cycles **3a** and 3**b**, showing the pyridyl and ethylene region of the *N*∩*N* linkers and the aromatic region of the *p*-cym ligands.

incorporating bpe and bpa could be explained by a difference of rigidity between bpe and bpa leading to different conformations of the metalla-cycles **1a**:**1b** and **3a**:**3b**. Moreover a broadening of the singlet associated to the ethane and ethylene protons of the bpa and bpe linkers suggests non-equivalent signals in metalla-cycles **1** and **3**. As previously reported,[14a] in metalla-cycle **6a** the asymmetry of the 9,10-anthraquinonato-1,4-diolato ligand after coordination to two metal centres does not affect the signals of the pyridyl protons nor the ethylene protons. However, in the case of metalla-cycle **6b**, an important broadening of the ethane signal of the bpa linkers is observed. This tends to confirm an effect of the rigidity of the *N*∩*N* linker on the geometrical conformation of the metalla-cycles, and the presence of two isomers in metalla-cycles **6**.

The cationic bpe-incorporating metalla-cycles **1a–7a** have been studied by electrospray ionisation mass spectrometry (ESI-MS). In particular, a peak corresponding to $[\mathbf{1a} + (CF_3SO_3)_2]^{2+}$ is observed in the ESI mass spectrum at *m*/*z* 916.1. This peak is unambiguously assigned on the basis of its characteristic Ru_4 isotope pattern. Concerning the new bpa-incorporating metalla-cycles **1b–7b**, an interesting fragmentation was observed. Peaks corresponding to [**CL**^{x} + bpa + CF_3SO_3 + 1] are observed in all mass spectra at *m*/*z* 919.1, 893.1, 960.1, 942.1, 993.1, 1043.1, 1093.1, respectively (Fig. 7).

The size of the metalla-cycles has been estimated using the HyperChem software.[26] As expected the simulations show an almost identical sizes for metalla-cycles **1–3** and **5–7**, while the size of metalla-cycle **4** is somewhere in between. The presence of bpe or bpa does not significantly modify the size, the bpa linkers,

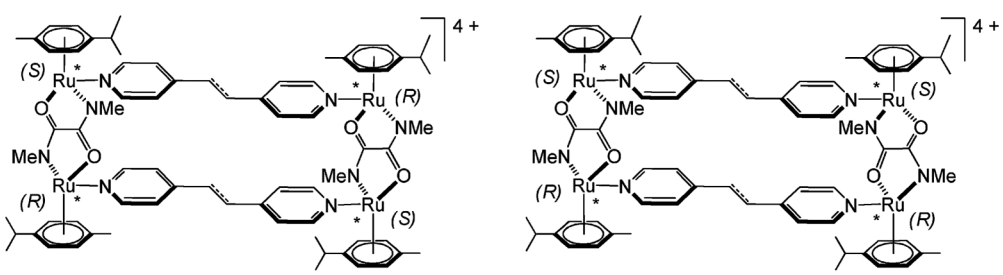

Fig. 5 Schematic representation of the two isomers of **1**.

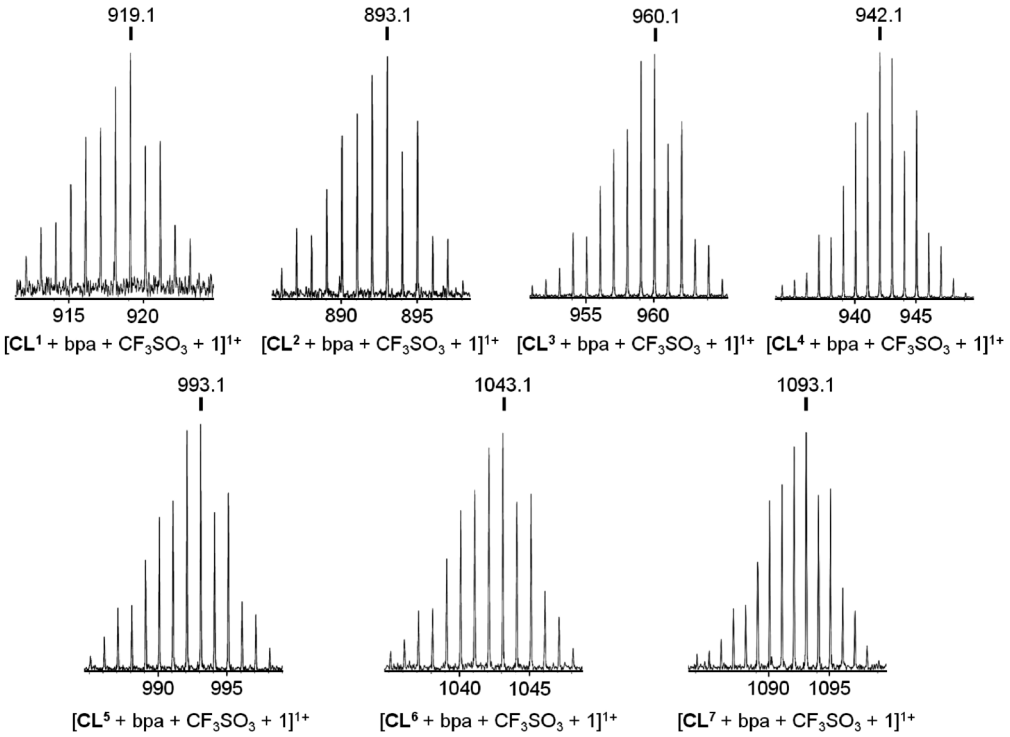

Fig. 7 ESI-MS of the peak envelopes corresponding to the fragmentation of [**1b–7b**][CF_3SO_3]$_4$.

however, offer more flexibility. Therefore, in this series, the size of the metalla-cycles is related to the *OO*∩*OO* and *NO*∩*NO* linkers. Models of the metalla-cycles are presented in Fig. 8, together with an estimation of the corresponding cavity sizes.

The difference of cavity sizes for the three groups of metalla-cycles (**1–3**; **4**; **5–7**), estimated by computational method, can be linked with previous results and in particular with the accommodation of small polycyclic aromatic hydrocarbon molecules into the hydrophobic cavity of metalla-cycles **5a–7a**.[14a,c] The hosting ability of these three metalla-cycles towards planar aromatic guest molecules such as pyrene, perylene and coronene was established using different spectroscopic methods.[14a,c] Strong association constants were estimated in solution for the corresponding host–guest systems, indicating a great potential as host systems for this kind of metalla-cycles. Similarly, Navarro and Barea have shown that the tetranuclear metalla-cycles [(η^6-*p*-cym)$_4$Ru$_4$(oxo)$_2$(4,4′-bipyridine)$_2$]$^{4+}$ and [(η^6-*p*-cym)$_4$Ru$_4$(oxo)$_2$(4,7-phenanthroline)$_2$]$^{4+}$ interact weakly with guanosine monophosphate (GMP) and adenosine monophosphate (AMP) in aqueous solution.[9] Therefore, we investigate the ability of metalla-cycles **1–7** to interact with guanine and guanosine in solution (50 : 50 DMSO-d_6 : D_2O). However, the ^{1}H NMR spectra of the metalla-cycles were not affected by gradual addition of these nucleotides, suggesting no in- or out-of-cavity interactions under these experimental conditions.

Antiproliferative activity

The antiproliferative activities of the water-soluble metalla-cycles containing the ligands 1,2-bis(4-pyridyl)ethylene (**1a–7a**) and 1,2-bis(4-pyridyl)ethane (**1b–7b**) were evaluated against the

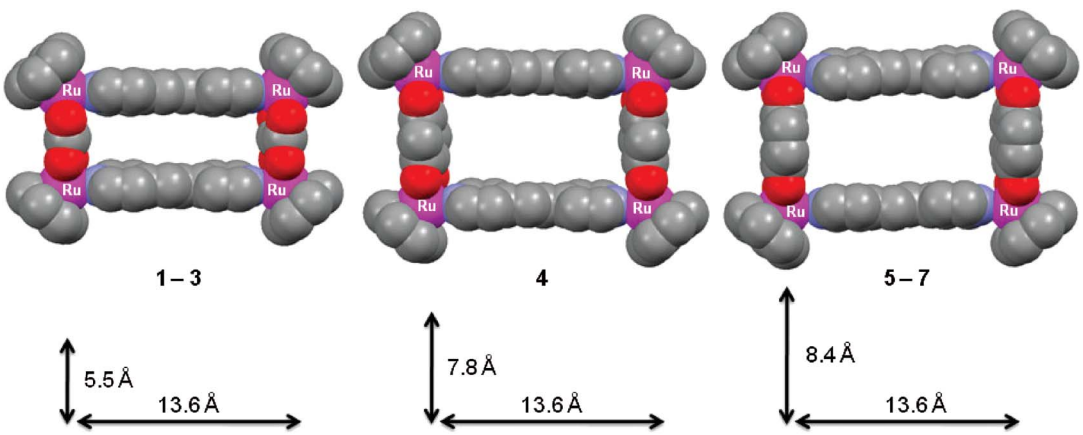

Fig. 8 Estimated sizes (Ru–Ru separations) of the metalla-cycles **1–7**.

Table 1 IC_{50} values and resistance factors (RFs) of complexes **1a–7b** in A2780 and A2780cisR cell lines and metalla-cycles **8–12**[9,10]

Complex	A2780 (IC_{50}, μM)	A2780cisR (IC_{50}, μM)	RF
1a	26.4 ± 1.0	112.7 ± 17.2	4.3
2a	4.2 ± 0.9	10.3 ± 2.6	2.5
3a	10.3 ± 1.2	23.3 ± 0.2	2.3
4a	10.3 ± 5.4	13.3 ± 6.1	1.3
5a	2.7 ± 1.0	2.5 ± 0.9	0.9
6a	9.4 ± 0.8	13.8 ± 3.6	1.5
7a	9.9 ± 1.8	8.5 ± 0.6	0.9
1b	35.5 ± 7.3	20.8 ± 5.3	0.6
2b	65.8 ± 9.6	75.3 ± 9.8	1.1
3b	144.7 ± 12.8	116.3 ± 9.2	0.8
4b	2.4 ± 1.1	5.9 ± 0.7	2.1
5b	2.6 ± 0.5	2.0 ± 0.3	0.7
6b	8.3 ± 0.2	7.6 ± 2.1	0.9
7b	17.5 ± 5.8	5.2 ± 1.4	0.3
8	19.0	4.6	0.2
9	15.0	8.3	0.6
10	0.8 ± 0.1	2.4 ± 0.1	3.0
11	0.2 ± 0.1	0.2 ± 0.1	1.0
12	3.3 ± 0.1	3.1 ± 0.1	0.9
Cisplatin	3.1	15.5	4.7

A2780 and A2780cisR ovarian cancer cell lines, and the results are presented in Table 1. IC_{50} values on A2780 and A2780cisR cancer cells of metalla-cycles $[(\eta^6\text{-}p\text{-cym})_4Ru_4(oxo)_2(4,4'\text{-bipyridine})_2]^{4+}$ (**8**), $[(\eta^6\text{-}p\text{-cym})_4Ru_4(oxo)_2(4,7\text{-phenanthroline})_2]^{4+}$ (**9**), $[(\eta^6\text{-}p\text{-cym})_4Ru_4(dobq)_2(4,7\text{-phenanthroline})_2]^{4+}$ (**10**), $[(\eta^6\text{-}p\text{-cym})_4Ru_4(donq)_2(4,7\text{-phenanthroline})_2]^{4+}$ (**11**), and $[(\eta^6\text{-}p\text{-cym})_4Ru_4(dcbq)_2(4,7\text{-phenanthroline})_2]^{4+}$ (**12**), previously published by Navarro and Barea are also given for comparison but were not re-evaluated in this study.[9,10] The molecular structures of these metalla-cycles (**8–12**) are presented in Fig. 9.

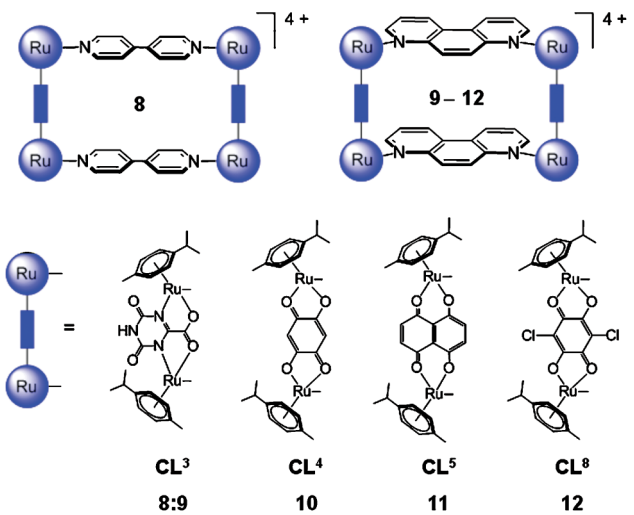

Fig. 9 Molecular structures of metalla-cycles **8–12**.[9,10]

All new metalla-cycles exhibit moderate to excellent activity with IC_{50} values in the range 2–35 μM, except for metalla-cycles **2b** and **3b** for which the antiproliferative activity is lower by at least a factor 2 (see Table 1). Moreover, the activities of the metalla-cycles are comparable to those of the metalla-assemblies **8**, **9** and **12**, but remain slightly less active than the phenanthroline derivatives **10** and **11**.[10] Phenanthroline is well known for its interaction with DNA, and it might explain the higher activity of the 4,7-phenanthroline metalla-cycles **10** and **11**.[27,28] Interestingly, metalla-cycle **1a** is 4 times more active on the non-resistant cisplatin cell line (A2780), while most complexes show an almost identical or even a better cytotoxicity on the cisplatin resistant cancer cell line (A2780cisR), as noted in Table 1. Overall, the average resistance factor (RF) value (RF = IC_{50}(A2780cisR)/IC_{50}(A2780)) is more or less 1, thus confirming that metalla-cycles display a different mode of action than that of cisplatin. A tendency often observed with arene ruthenium and arene osmium metal-based drugs.[29]

In recent years, a large number of cationic polynuclear ruthenium complexes have been evaluated as putative anticancer agents.[30] The high charge of these complexes not only facilitates uptake to cancer cells,[29a,31] it generates good DNA binding systems.[30] DNA remains the primary target for arene ruthenium drugs,[32] and as previously shown arene ruthenium metalla-cycles are excellent DNA binding systems.[16b,28] Therefore, the good cytotoxicity observed here for metalla-cycles **1–7** is possibly related with the DNA binding affinities of these systems. Indeed, it appears that metalla-cycles with multiple π-aromatic groups (**4–7**) and those offering more flexibility (**4b–7b**) are more active against the ovarian cancer cell lines than the smaller assemblies (**1–3**). However, despite this potential interaction with DNA, other biological targets cannot be excluded and other mechanisms of action can also play an important role in the biological activity of these metalla-cycles.

Conclusion

A series of cationic metalla-cycles based on arene ruthenium units have been prepared and characterised by different spectroscopic methods. These water-soluble compounds were screened for *in vitro* anticancer activity against the A2780 and A2780cisR ovarian cancer cell lines and all metalla-cycles exhibit moderate to excellent activity. Moreover some metalla-cycles were found to be more active on the cisplatin resistant cancer cell line than on the cisplatin sensitive line, suggesting a different biological mechanism than that of cisplatin.

Experimental

General details

The $[Ru(\eta^6\text{-}p\text{-cym})Cl_2]_2$,[33] the dinuclear arene ruthenium complexes $[Ru_2(\eta^6\text{-}p\text{-cym})_2(OO\cap OO)Cl_2]$ ($OO\cap OO$ = ox,[6b] dobq,[15a] donq,[15b] doaq,[34] dotq[14a]), $[Ru_2(\eta^6\text{-}p\text{-cym})_2(NO\cap NO)Cl_2]$ ($NO\cap NO$ = oxo[9]) and the metalla-cycles **2a**,[14b] **4a**,[17] **5a**,[14b] **6a**,[14c] and **7a**[14c] were prepared according to published methods. All other reagents were commercially available (Sigma-Aldrich) and used as received. The ^1H and $^{13}C\{^1H\}$ NMR spectra were recorded on a Bruker AMX 400 spectrometer using the residual protonated solvent as internal standard. Infrared spectra were recorded as KBr pellets on a Perkin-Elmer FTIR 1720 X spectrometer. UV-visible absorption spectra were recorded on an Uvikon 930 spectrophotometer using precision cells made of quartz (1 cm). Electrospray ionisation mass spectra were obtained in positive-ion mode on a Bruker FTMS 4.7T BioAPEX II mass spectrometer. Microanalysis was performed by the Mikroelementarisches Laboratorium, ETH Zürich (Switzerland).

Synthesis of metalla-clip CL^{1}Cl$_2$

n-BuLi (0.30 mL, 0.48 mmol) was added to a solution of *N*,*N*′-dimethyloxamide (oxa-H$_2$) (27.9 mg, 0.24 mmol) in THF (15 mL) at −78 °C. The reaction mixture was stirred and warmed to room temperature (2 h). Then the mixture was added to a solution of [Ru(η^6-*p*-cym)Cl$_2$]$_2$ (146.9 mg, 0.24 mmol) in THF (5 mL), and stirred overnight. The solvent was evaporated *in vacuo* and the residue washed several times with water, and finally with diethyl ether and pentane before being dried.

CL^{1}Cl$_2$: Yield: 96 mg (61%). IR: ν (cm^{-1}): 3060 (w, CH$_{aryl}$), 1609 (s, C═O). ^{1}H NMR (400 MHz, CD$_2$Cl$_2$, 298 K): δ (ppm) = 5.35 (d, ^3J = 5.7 Hz, 2 H, H$_{ar}$), 5.32 (d, ^3J = 5.8 Hz, 2 H, H$_{ar}$), 5.26 (d, 2 H, H$_{ar}$), 5.06 (d, 2 H, H$_{ar}$), 3.27 (s, 6 H, CH$_3$), 2.71 (sept, ^3J = 2.7 Hz, 2 H, C*H*(CH$_3$)$_2$), 2.12 (s, 6 H, CH$_3$), 1.21 (d, 6 H, CH(C*H*$_3$)$_2$), 1.19 (d, 6 H, CH(C*H*$_3$)$_2$). ^{13}C{^{1}H} NMR (100 MHz, CD$_2$Cl$_2$, 298 K): δ (ppm) = 170.3 (CO), 100.8 (C$_{ar}$), 95.8 (C$_{ar}$), 81.9 (CH$_{ar}$), 81.3 (CH$_{ar}$), 80.9 (CH$_{ar}$), 79.6 (CH$_{ar}$), 38.0 (CH$_3$), 31.5 (*C*H(CH$_3$)$_2$), 22.6 (CH(*C*H$_3$)$_2$), 22.5 (CH(*C*H$_3$)$_2$), 18.7 (CH$_3$). UV-vis (1.0 × 10^{-5} M, CH$_2$Cl$_2$): λ_{max} 306 nm (ε = 2.96 × 10^5 M^{-1} cm^{-1}). Elemental Analysis (%): Calc. for C$_{24}$H$_{34}$Cl$_2$N$_2$O$_2$Ru$_2$ (655.6): C, 43.97; H, 5.23; N, 4.27; Found: C, 43.86; H, 5.22; N, 4.27%.

Synthesis of metalla-cycles [1a][CF$_3$SO$_3$]$_4$, [3a][CF$_3$SO$_3$]$_4$ and [1b–7b][CF$_3$SO$_3$]$_4$

AgCF$_3$SO$_3$ (149.0 mg, 0.58 mmol) was added to a suspension of [Ru$_2$(η^6-*p*-cym)$_2$(*OO*∩*OO*)Cl$_2$] or [Ru$_2$(η^6-*p*-cym)$_2$(*NO*∩*NO*)Cl$_2$] (oxa (**1a**, **1b**; 190.1 mg), ox (**2b**; 182.6 mg), oxo (**3a**, **3b**; 202.6 mg), dobq (**4b**; 196.9 mg), donq (**5b**; 211.4 mg), doaq (**6b**; 225.9 mg), dotq (**7b**; 240.4 mg); 0.29 mmol) in methanol (100 mL) at 60 °C and stirred for 12 h, followed by filtration to remove AgCl. Then, 1,2-bis(4-pyridyl)ethylene (**1a**, **3a**; 52.8 mg, 0.29 mmol) or 1,2-bis(4-pyridyl)ethane (**1b–7b**; 53.4 mg, 0.29 mmol) was added to the filtrate. The solution was stirred at 60 °C for 24 h. The solvent was removed and the residue extracted with dichloromethane. The filtrate was concentrated to about 2 mL and diethyl ether added. The precipitate was washed with diethyl ether (3 × 50 mL) and pentane (3 × 50 mL) and dried *in vacuo* to give the corresponding product as powder.

[**1a**][CF$_3$SO$_3$]$_4$: Yield: 200 mg (65%). IR: ν (cm^{-1}): 3070 (m, CH$_{ar}$), 1616 (s, C═O), 1256 (s, CF). ^{1}H NMR (400 MHz, CD$_3$CN, 298 K): δ (ppm) = 7.96 (br, 4 H, H$_\alpha$), 7.94 (br, 4 H, H$_\alpha$), 7.53 (br, 4 H, H$_\beta$), 7.51 (br, 4 H, H$_\beta$), 7.44 (br, 4 H, H$_{C=C}$), 5.87 (m, 4 H, H$_{ar}$), 5.77 (m, 4 H, H$_{ar}$), 5.38 (m, 4 H, H$_{ar}$), 5.30 (m, 4 H, H$_{ar}$), 3.51 (s, 12 H, CH$_3$), 2.75 (m, 4 H, C*H*(CH$_3$)$_2$), 1.96 (s, 12 H, CH$_3$), 1.30 (m, 24 H, CH(C*H*$_3$)$_2$). ^{13}C{^{1}H} NMR (100 MHz, CD$_3$CN, 298 K): δ (ppm) = 170.6 (CO), 152.8 (CH$_\alpha$), 145.8 (C$_{pyr}$), 132.0 (HC═CH), 123.4 (CH$_\beta$), 102.4 (C$_{ar}$), 99.7 (C$_{ar}$), 86.5 (CH$_{ar}$), 84.5 (CH$_{ar}$), 81.7 (CH$_{ar}$), 78.4 (CH$_{ar}$), 37.9 (CH$_3$), 31.0 (*C*H(CH$_3$)$_2$), 21.6 (CH(*C*H$_3$)$_2$), 16.9 (CH$_3$). UV-vis (1.0 × 10^{-5} M, CH$_2$Cl$_2$): λ_{max} 269 nm (ε = 3.15 × 10^5 M^{-1} cm^{-1}), λ_{max} 340 nm (ε = 0.61 × 10^5 M^{-1} cm^{-1}). Elemental Analysis (%): Calc. for C$_{76}$H$_{88}$F$_{12}$N$_8$O$_{16}$Ru$_4$S$_4$ (2130.1): C, 42.85; H, 4.16; N, 5.26; Found: C, 42.76; H, 4.30; N, 5.18%.

[**3a**][CF$_3$SO$_3$]$_4$: Yield: 208 mg (65%). IR: ν (cm^{-1}): 3077 (m, CH$_{ar}$), 1712 (s, C═N), 1612 (s, C═O), 1259 (s, CF). ^{1}H NMR (400 MHz, CD$_3$CN, 298 K): δ (ppm) = 9.98 (s, 2 H, NH), 7.97 (br, 4 H, H$_\alpha$), 7.94 (br, 4 H, H$_\alpha$), 7.56 (br, 4 H, H$_\beta$), 7.53 (br, 4 H, H$_\beta$), 7.40 (br, 4 H, H$_{C=C}$), 6.06 (m, 4 H, H$_{ar}$), 6.03 (m, 4 H, H$_{ar}$), 5.94 (m, 4 H, H$_{ar}$), 5.50 (m, 4 H, H$_{ar}$), 2.75 (m, 4 H, C*H*(CH$_3$)$_2$), 1.96 (s, 12 H, CH$_3$), 1.24 (m, 12 H, CH(C*H*$_3$)$_2$), 1.15 (m, 12 H, CH(C*H*$_3$)$_2$). ^{13}C{^{1}H} NMR (100 MHz, CD$_3$CN, 298 K): δ (ppm) = 178.9 (CO), 162.4 (CN), 154.6 (CH$_\alpha$), 146.1 (C$_{pyr}$), 132.1 (HC═CH), 124.0 (CH$_\beta$), 106.0 (C$_{ar}$), 99.4 (C$_{ar}$), 83.9 (CH$_{ar}$), 83.7 (CH$_{ar}$), 83.6 (CH$_{ar}$), 80.7 (CH$_{ar}$), 30.9 (*C*H(CH$_3$)$_2$), 21.5 (CH(*C*H$_3$)$_2$), 17.0 (CH$_3$). UV-vis (1.0 × 10^{-5} M, CH$_2$Cl$_2$): λ_{max} 265 nm (ε = 3.00 × 10^5 M^{-1} cm^{-1}), λ_{max} 331 nm (ε = 0.51 × 10^5 M^{-1} cm^{-1}). Elemental Analysis (%): Calc. for C$_{76}$H$_{78}$F$_{12}$N$_{10}$O$_{20}$Ru$_4$S$_4$ (2212.0): C, 41.27; H, 3.55; N, 6.33; Found: C, 41.20; H, 3.66; N, 6.22%.

[**1b**][CF$_3$SO$_3$]$_4$: Yield: 191 mg (62%). IR: ν (cm^{-1}): 3073 (m, CH$_{ar}$), 1620 (s, C═O), 1259 (s, CF). ^{1}H NMR (400 MHz, CD$_3$CN, 298 K): δ (ppm) = 7.89 (d, 4 H, ^3J = 5.1 Hz, H$_\alpha$), 7.67 (d, 4 H, H$_\alpha$), 7.09 (d, 4 H, ^3J = 5.4 Hz, H$_\beta$), 6.84 (d, 4 H, H$_\beta$), 5.81 (d, 4 H, ^3J = 5.8 Hz, H$_{ar}$), 5.73 (d, 4 H, ^3J = 6.2 Hz, H$_{ar}$), 5.45 (d, 4 H, H$_{ar}$), 5.31 (d, 4 H, H$_{ar}$), 3.46 (s, 12 H, CH$_3$), 3.36 (s, 8 H, H$_{bpa}$), 2.70 (sept, 4 H, ^3J = 8.2 Hz, C*H*(CH$_3$)$_2$), 1.81 (s, 12 H, CH$_3$), 1.78 (d, 12 H, CH(C*H*$_3$)$_2$), 1.22 (d, 12 H, CH(C*H*$_3$)$_2$). ^{13}C{^{1}H} NMR (100 MHz, CD$_3$CN, 298 K): δ (ppm) = 170.1 (CO), 153.8 (CH$_\alpha$), 153.5 (CH$_\alpha$), 152.8 (C$_{pyr}$), 150.6 (C$_{pyr}$), 129.1 (CH$_\beta$), 128.0 (CH$_\beta$), 103.5 (C$_{ar}$), 99.8 (C$_{ar}$), 86.7 (CH$_{ar}$), 84.7 (CH$_{ar}$), 82.6 (CH$_{ar}$), 79.3 (CH$_{ar}$), 38.5 (CH$_3$), 36.0 (CH$_{bpa}$), 22.5 (*C*H(CH$_3$)$_2$), 22.4 (CH(*C*H$_3$)$_2$), 18.1 (CH$_3$). UV-vis (1.0 × 10^{-5} M, CH$_2$Cl$_2$): λ_{max} 727 nm (ε = 3.08 × 10^5 M^{-1} cm^{-1}), λ_{max} 342 nm (ε = 0.65 × 10^5 M^{-1} cm^{-1}). Elemental Analysis (%): Calc. for C$_{76}$H$_{92}$F$_{12}$N$_8$O$_{16}$Ru$_4$S$_4$ (2134.1): C, 42.77; H, 4.35; N, 5.25; Found: C, 42.68; H, 4.48; N, 5.16%.

[**2b**][CF$_3$SO$_3$]$_4$: Yield: 205 mg (68%). IR: ν (cm^{-1}): 3070 (m, CH$_{ar}$), 1613 (s, C═O), 1259 (s, CF). ^{1}H NMR (400 MHz, CD$_3$CN, 298 K): δ (ppm) = 7.74 (d, 8 H, ^3J = 6.3 Hz, H$_\alpha$), 7.00 (d, 8 H, H$_\beta$), 5.82 (d, 8 H, ^3J = 6.1 Hz, H$_{ar}$), 5.69 (d, 8 H, H$_{ar}$), 3.25 (s, 8 H, H$_{bpa}$), 2.80 (sept, 4 H, ^3J = 2.5 Hz, C*H*(CH$_3$)$_2$), 2.15 (s, 12 H, CH$_3$), 1.30 (d, 24 H, CH(C*H*$_3$)$_2$). ^{13}C{^{1}H} NMR (100 MHz, CD$_3$CN, 298 K): δ (ppm) = 173.0 (CO), 151.8 (CH$_\alpha$), 145.2 (C$_{pyr}$), 127.3 (CH$_\beta$), 100.2 (C$_{ar}$), 98.7 (C$_{ar}$), 84.9 (CH$_{ar}$), 83.7 (CH$_{ar}$), 33.0 (CH$_{bpa}$), 32.2 (*C*H(CH$_3$)$_2$), 22.7 (CH(*C*H$_3$)$_2$), 19.2 (CH$_3$). UV-vis (1.0 × 10^{-5} M, CH$_2$Cl$_2$): λ_{max} 267 nm (ε = 2.89 × 10^5 M^{-1} cm^{-1}), λ_{max} 340 nm (ε = 0.45 × 10^5 M^{-1} cm^{-1}). Elemental Analysis (%): Calc. for C$_{72}$H$_{80}$F$_{12}$N$_4$O$_{20}$Ru$_4$S$_4$ (2081.9): C, 41.54; H, 3.87; F, 10.95; N, 2.69; Found: C, 41.45; H, 4.03; N, 2.65%.

[**3b**][CF$_3$SO$_3$]$_4$: Yield: 251 mg (78%). IR: ν (cm^{-1}): 3077 (m, CH$_{ar}$), 1709 (s, C═N), 1594 (s, C═O), 1260 (s, CF). ^{1}H NMR (400 MHz, CD$_3$CN, 298 K): δ (ppm) = 9.98 (s, 2 H, NH), 8.02 (m, 4 H, H$_\alpha$), 7.42 (m, 4 H, H$_\alpha$), 7.06 (m, 4 H, H$_\beta$), 6.92 (m, 4 H, H$_\beta$), 6.02 (m, 8 H, H$_{ar}$), 5.90 (m, 4 H, H$_{ar}$), 5.80 (m, 4 H, H$_{ar}$), 3.24 (br, 8 H, H$_{bpa}$), 2.73 (m, 4 H, C*H*(CH$_3$)$_2$), 2.09 (s, 12 H, CH$_3$), 1.23 (m, 12 H, CH(C*H*$_3$)$_2$), 1.15 (m, 12 H, CH(C*H*$_3$)$_2$). ^{13}C{^{1}H} NMR (100 MHz, CD$_3$CN, 298 K): δ (ppm) = 178.9 (CO), 162.4 (CN), 154.6 (CH$_\alpha$), 146.2 (C$_{pyr}$), 124.1 (CH$_\beta$), 106.1 (C$_{ar}$), 99.3 (C$_{ar}$), 84.0 (CH$_{ar}$), 83.8 (CH$_{ar}$), 83.7 (CH$_{ar}$), 83.6 (CH$_{ar}$), 30.9 (*C*H(CH$_3$)$_2$), 21.5 (CH(*C*H$_3$)$_2$), 17.1 (CH$_3$). UV-vis (1.0 × 10^{-5} M, CH$_2$Cl$_2$): λ_{max} 269 nm (ε = 2.81 × 10^5 M^{-1} cm^{-1}), λ_{max} 374 nm (ε = 0.20 × 10^5 M^{-1} cm^{-1}). Elemental Analysis (%): Calc. for C$_{76}$H$_{82}$F$_{12}$N$_{10}$O$_{20}$Ru$_4$S$_4$ (2216.0): C, 41.19; H, 3.73; N, 6.32; Found: C, 41.15; H, 3.87; N, 6.23%.

[**4b**][CF$_3$SO$_3$]$_4$: Yield: 259 mg (82%). IR: ν (cm^{-1}): 3068 (m, CH$_{ar}$), 1598 (s, C═O), 1260 (s, CF). ^{1}H NMR (400 MHz, CD$_3$CN, 298 K): δ (ppm) = 7.78 (d, ^3J = 6.1 Hz, 8 H, H$_\alpha$), 7.13 (d, 8 H,

H_β), 5.92 (d, ^3J = 6.3 Hz, 8 H, H_{ar}), 5.86 (d, 8 H, H_{ar}), 5.48 (s, 4 H, H_{dobq}), 3.26 (s, 8 H, H_{bpa}), 2.85 (sept, ^3J = 2.5 Hz, 4 H, C*H*(CH_3)$_2$), 2.10 (s, 12 H, CH_3), 1.30 (d, 24 H, CH(C*H*$_3$)$_2$). $^{13}C\{^1H\}$ NMR (100 MHz, CD_3CN, 298 K): δ (ppm) = 171.4 (CO), 153.2 (CH_α), 150.7 (C_{pyr}), 130.1 (CH_β), 114.6 (CH_{dobq}), 108.2 (C_{dobq}), 102.1 (C_{ar}), 99.8 (C_{ar}), 84.2 (CH_{ar}), 84.0 (CH_{ar}), 29.3 (CH_{bpa}), 30.0 (*C*H(CH_3)$_2$), 20.9(CH(*C*H$_3$)$_2$), 17.4 (CH_3). UV-vis (1.0×10^{-5} M, CH_2Cl_2): λ_{max} 265 nm ($\varepsilon = 3.01 \times 10^5$ M^{-1} cm^{-1}), λ_{max} 317 nm ($\varepsilon = 0.46 \times 10^5$ M^{-1} cm^{-1}), λ_{max} 510 nm ($\varepsilon = 0.43 \times 10^5$ M^{-1} cm^{-1}). Elemental Analysis (%): Calc. for $C_{80}H_{84}F_{12}N_4O_{20}Ru_4S_4$ (2182.1): C, 44.03; H, 3.88; N, 2.57; Found: C, 43.92; H, 4.00; N, 2.50%.

[**5b**][CF_3SO_3]$_4$: Yield: 248 mg (75%). IR: ν (cm^{-1}): 3070 (m, CH_{ar}), 1619 (s, C═O), 1259 (s, CF). ^{1}H NMR (400 MHz, CD_3CN, 298 K): δ (ppm) = 7.94 (d, ^3J = 6.3 Hz, 8 H, H_α), 7.03 (d, 8 H, H_β), 6.96 (s, 8 H, H_{donq}), 5.66 (d, ^3J = 6.3 Hz, 8 H, H_{ar}), 5.44 (d, 8 H, H_{ar}), 3.21 (s, 8 H, H_{bpa}), 2.82 (sept, ^3J = 2.1 Hz, 4 H, C*H*(CH_3)$_2$), 2.10 (s, 12 H, CH_3), 1.30 (d, 24 H, CH(C*H*$_3$)$_2$). $^{13}C\{^1H\}$ NMR (100 MHz, CD_3CN, 298 K): δ (ppm) = 170.3 (CO), 152.9 (CH_α), 151.9 (C_{pyr}), 137.2 (CH_β), 125.8 (CH_{donq}), 111.3 (C_{donq}), 103.4 (C_{ar}), 99.0 (C_{ar}), 83.7 (CH_{ar}), 82.8 (CH_{ar}), 31.1 (CH_{bpa}), 30.6 (*C*H(CH_3)$_2$), 21.4 (CH(*C*H$_3$)$_2$), 16.5 (CH_3). UV-vis (1.0×10^{-5} M, CH_2Cl_2): λ_{max} 266 nm ($\varepsilon = 2.99 \times 10^5$ M^{-1} cm^{-1}), λ_{max} 327 nm ($\varepsilon = 0.30 \times 10^5$ M^{-1} cm^{-1}), λ_{max} 454 nm ($\varepsilon = 0.22 \times 10^5$ M^{-1} cm^{-1}), λ_{max} 720 nm ($\varepsilon = 0.08 \times 10^5$ M^{-1} cm^{-1}). Elemental Analysis (%): Calc. for $C_{88}H_{88}F_{12}N_4O_{20}Ru_4S_4$ (2282.2): C, 46.31; H, 3.89; F, 9.99; N, 2.45; Found: C, 46.16; H, 3.99; N, 2.39%.

[**6b**][CF_3SO_3]$_4$: Yield: 266 mg (77%). IR: ν (cm^{-1}): 3070 (m, CH_{ar}), 1618 (s, C═O), 1260 (s, CF). ^{1}H NMR (400 MHz, CD_3CN, 298 K): δ (ppm) = 8.46 (d, ^3J = 6.1 Hz, 8 H, H_α), 8.01 (d, 8 H, H_β), 7.90 (m, 4 H, H_{doaq}), 7.06 (s, 4 H, H_{doaq}), 5.78 (d, ^3J = 6.3 Hz, 4 H, H_{ar}), 5.73 (d, ^3J = 6.1 Hz, 4 H, H_{ar}), 5.54 (d, 4 H, H_{ar}), 5.50 (d, 4 H, H_{ar}), 3.21 (br, 8 H, H_{bpa}), 2.92 (sept, ^3J = 2.3 Hz, 4 H, C*H*(CH_3)$_2$), 2.11 (s, 12 H, CH_3), 1.34 (d, 12 H, CH(C*H*$_3$)$_2$), 1.30 (d, 12 H, CH(C*H*$_3$)$_2$). $^{13}C\{^1H\}$ NMR (100 MHz, CD_3CN, 298 K): δ (ppm) = 171.5 (CO), 170.7 (CO), 155.4 (CH_α), 151.9 (C_{pyr}), 139.9 (CH_{doaq}), 138.3 (CH_β), 136.6 (CH_{doaq}), 134.3 (C_{doaq}), 132.0 (C_{doaq}), 128.2 (CH_{doaq}), 104.7 (C_{ar}), 100.3 (C_{ar}), 85.4 (CH_{ar}), 84.8 (CH_{ar}), 83.9 (CH_{ar}), 82.0 (CH_{ar}), 29.2 (CH_{bpa}), 31.2 (*C*H(CH_3)$_2$), 21.2 (CH(*C*H$_3$)$_2$), 21.0 (CH(*C*H$_3$)$_2$), 17.0 (CH_3). UV-vis (1.0×10^{-5} M, CH_2Cl_2): λ_{max} 264 nm ($\varepsilon = 3.01 \times 10^5$ M^{-1} cm^{-1}), λ_{max} 324 nm ($\varepsilon = 0.32 \times 10^5$ M^{-1} cm^{-1}), λ_{max} 417 nm ($\varepsilon = 0.25 \times 10^5$ M^{-1} cm^{-1}), λ_{max} 683 nm ($\varepsilon = 0.13 \times 10^5$ M^{-1} cm^{-1}). Elemental Analysis (%): Calc. for $C_{96}H_{92}F_{12}N_4O_{20}Ru_4S_4$ (2382.3): C, 48.40; H, 3.89; N, 2.35; Found: C, 48.22; H, 4.001; N, 2.30%.

[**7b**][CF_3SO_3]$_4$: Yield: 255 mg (71%). IR: ν (cm^{-1}): 3068 (m, CH_{ar}), 1612 (s, C═O), 1260 (s, CF). ^{1}H NMR (400 MHz, CD_3CN, 298 K): δ (ppm) = 8.53 (d, ^3J = 6.8 Hz, 8 H, H_α), 7.97 (d, ^3J = 8.4 Hz, 8 H, H_{dotq}), 7.89 (d, 8 H, H_β), 6.88 (d, 8 H, H_{dotq}), 5.85 (d, ^3J = 6.1 Hz, 8 H, H_{ar}), 5.61 (d, 8 H, H_{ar}), 3.33 (s, 8 H, H_{bpa}), 3.00 (sept, ^3J = 2.5 Hz, 4 H, C*H*(CH_3)$_2$), 2.12 (s, 12 H, CH_3), 1.37 (d, 24 H, CH(C*H*$_3$)$_2$). $^{13}C\{^1H\}$ NMR (100 MHz, CD_3CN, 298 K): δ (ppm) = 170.4 (CO), 153.1 (CH_α), 152.5 (C_{pyr}), 139.1 (CH_β), 134.7 (CH_{dotq}), 133.6 (C_{dotq}), 133.5 (C_{dotq}), 132.4 (CH_{dotq}), 100.2 (C_{ar}), 96.0 (C_{ar}), 84.7 (CH_{ar}), 83.9 (CH_{ar}), 32.3 (CH_{bpa}), 31.3 (*C*H(CH_3)$_2$), 19.8 (CH(*C*H$_3$)$_2$), 17.0 (CH_3). UV-vis (1.0×10^{-5} M, CH_2Cl_2): λ_{max} 267 nm ($\varepsilon = 3.07 \times 10^5$ M^{-1} cm^{-1}), λ_{max} 327 nm ($\varepsilon = 0.44 \times 10^5$ M^{-1} cm^{-1}), λ_{max} 379 nm ($\varepsilon = 0.38 \times 10^5$ M^{-1} cm^{-1}), λ_{max} 409 nm ($\varepsilon = 0.29 \times 10^5$ M^{-1} cm^{-1}), λ_{max} 588 nm ($\varepsilon = 0.16 \times 10^5$ M^{-1} cm^{-1}), λ_{max} 636 nm ($\varepsilon = 0.19 \times 10^5$ M^{-1} cm^{-1}). Elemental Analysis (%): Calc. for $C_{104}H_{96}F_{12}N_4O_{20}Ru_4S_4$ (2482.4): C, 50.32; H, 3.90; N, 2.26; Found: C, 50.11; H, 3.97; N, 2.20%.

Cell culture and inhibition of cell growth

Human A2780 and A2780cisR ovarian carcinoma cells were obtained from the European Centre of Cell Cultures (ECACC, Salisbury, UK) and maintained in culture as described by the provider. The cells were routinely grown in RPMI 1640 medium with GlutaMAX™ containing 10% foetal calf serum (FCS) and antibiotics (penicillin and streptomycin) at 37 °C and 5% CO_2. For the evaluation of growth inhibition tests, the cells were seeded in 96-well plates (25×10^3 cells per well) and grown for 24 h in complete medium. Solutions of the compounds were applied by diluting a freshly prepared stock solution of the corresponding compound in RPMI medium. The stock solutions of metal complexes were prepared by dissolving the compounds in 0.5 mL of DMSO to reach a concentration of 10^{-2} M. They were then diluted in RPMI medium and added to the wells (100 µL) to obtain a final concentration ranging between 0 and 150 µM for 72 h incubation. DMSO at comparable concentrations did not show any effects on cell cytotoxicity. Following drug exposure, 3-(4,5-dimethylthiazol-2-yl)-2,5-diphenyltetrazolium bromide (MTT) was added to the cells at a final concentration of 0.25 mg mL^{-1} and incubated for 2 h, then the culture medium was aspirated and the violet formazan (artificial chromogenic precipitate of the reduction of tetrazolium salts by dehydrogenases and reductases) dissolved in DMSO. The optical density of each well (96-well plates) was quantified three times in tetraplicates at 540 nm using a multiwell plate reader (iEMS Reader MF, Labsystems, US), and the percentage of surviving cells was calculated from the ratio of absorbance of treated to untreated cells. The half maximal inhibitory concentration (IC_{50}) values for the inhibition of cell growth were determined by fitting the plot of the logarithmic percentage of surviving cells against the logarithm of the drug concentration using a linear regression function and the values obtained are reported in Table 1.

Acknowledgements

We thank Johnson Matthey Technology Centre for a generous loan of ruthenium chloride hydrate and Dr Julien Furrer for his help with NMR experiments.

References

1 (*a*) J.-M. Lehn, *Angew. Chem., Int. Ed. Engl.*, 2008, **29**, 1304–1319; (*b*) D. J. Cram, *Science*, 1983, **219**, 1177–1183.
2 E. Maverick and D. J. Cram, in *Comprehensive Supramolecular Chemistry*, ed, J. L. Atwood, J. E. D. Davis, D. D. MacNicol and F. Vögtle, Pergamon, Oxford, 1996, vol. 1, pp. 213–243.
3 (*a*) D. L. Caulder and K. N. Raymond, *Acc. Chem. Res.*, 1999, **32**, 975–982; (*b*) B. H. Northrop, H.-B. Yang and P. J. Stang, *Chem. Commun.*, 2008, 5896–5908; (*c*) M. Fujita, M. Tominaga, A. Hori and B. Therrien, *Acc. Chem. Res.*, 2005, **38**, 369–378.
4 R. H. Fish, *Coord. Chem. Rev.*, 1999, **185**, 569–584.
5 (*a*) T. Habereder, M. Warchhold, H. Nöth and K. Severin, *Angew. Chem., Int. Ed.*, 1999, **38**, 3225–3228; (*b*) T. B. Rauchfuss and K. Severin, in *Organic Nanostructures*, ed. J. L. Atwood and J. W. Steed, Wiley-VCH, Weinheim, 2008, pp. 179–203.
6 (*a*) H. Yan, G. Süss-Fink, A. Neels and H. Stoeckli-Evans, *J. Chem. Soc., Dalton Trans.*, 1997, 4345–4350; (*b*) P. Annen, S. Schildberg and W. S. Sheldrick, *Inorg. Chim. Acta*, 2000, **307**, 115–124; (*c*) S.

Shanmugaraju, A. K. Bar, S. A. Joshi, Y. P. Patil and P. S. Mukherjee, *Organometallics*, 2011, **30**, 1951–1960.
7 S. Mirtschin, A. Slabon-Turski, R. Scopelliti, A. H. Velders and K. Severin, *J. Am. Chem. Soc.*, 2010, **132**, 14004–14005.
8 (*a*) L. Mimassi, C. Guyard-Duhayon, M. N. Rager and H. Amouri, *Inorg. Chem.*, 2004, **43**, 6644–6649; (*b*) K. Severin, *Coord. Chem. Rev.*, 2003, **245**, 3–10.
9 F. Linares, M. A. Galindo, S. Galli, M. A. Romero, J. A. R. Navarro and E. Barea, *Inorg. Chem.*, 2009, **48**, 7413–7420.
10 F. Linares, E. Q. Procopio, M. A. Galindo, M. A. Romero, J. A. R. Navarro and E. Barea, *CrystEngComm*, 2010, **12**, 2343–2346.
11 N. P. E. Barry, F. Edafe, P. J. Dyson and B. Therrien, *Dalton Trans.*, 2010, **39**, 2816–2820.
12 (*a*) G. Gasser, I. Ott and N. Metzler-Nolte, *J. Med. Chem.*, 2011, **54**, 3–25; (*b*) G. Süss-Fink, *Dalton Trans.*, 2010, **39**, 1673–1688; (*c*) Y. K. Yan, M. Melchart, A. Habtemariam and P. J. Sadler, *Chem. Commun.*, 2005, 4764–4776; (*d*) C. G. Hartinger and P. J. Dyson, *Chem. Soc. Rev.*, 2009, **38**, 391–401.
13 B. Therrien, *Eur. J. Inorg. Chem.*, 2009, 2445–2453.
14 (*a*) N. P. E. Barry, J. Furrer and B. Therrien, *Helv. Chim. Acta*, 2010, **93**, 1313–1328; (*b*) N. P. E. Barry and B. Therrien, *Inorg. Chem. Commun.*, 2009, **12**, 465–468; (*c*) N. P. E. Barry, J. Furrer, J. Freudenreich, G. Süss-Fink and B. Therrien, *Eur. J. Inorg. Chem.*, 2010, 725–728.
15 (*a*) B. Therrien, G. Süss-Fink, P. Govindaswamy, A. K. Renfrew and P. J. Dyson, *Angew. Chem., Int. Ed.*, 2008, **47**, 3773–3776; (*b*) N. P. E. Barry and B. Therrien, *Eur. J. Inorg. Chem.*, 2009, 4695–4700; (*c*) J. Freudenreich, N. P. E. Barry, G. Süss-Fink and B. Therrien, *Eur. J. Inorg. Chem.*, 2010, 2400–2405; (*d*) A. Pitto-Barry, N. P. E. Barry, O. Zava, R. Deschenaux, P. J. Dyson and B. Therrien, *Chem.–Eur. J.*, 2011, **17**, 1966–1971.
16 (*a*) N. P. E. Barry, O. Zava, P. J. Dyson and B. Therrien, *Aust. J. Chem.*, 2010, **63**, 1529–1537; (*b*) N. P. E. Barry, N. H. Abd Karim, R. Vilar and B. Therrien, *Dalton Trans.*, 2009, 10717–10719; (*c*) N. P. E. Barry, M. Austeri, J. Lacour and B. Therrien, *Organometallics*, 2009, **28**, 4894–4897; (*d*) N. P. E. Barry, P. Govindaswamy, J. Furrer, G. Süss-Fink and B. Therrien, *Inorg. Chem. Commun.*, 2008, **11**, 1300–1303.
17 J. Mattsson, P. Govindaswamy, A. K. Renfrew, P. J. Dyson, P. Štěpnička, G. Süss-Fink and B. Therrien, *Organometallics*, 2009, **28**, 4350–4357.
18 D. Astruc, *Chimie organométallique*, EDP Sciences: Les Ulis, 2000, 31–54.
19 A. Pitto-Barry, N. P. E. Barry, O. Zava, R. Deschenaux and B. Therrien, *Chem.–Asian J.*, DOI: 10.1002/asia.201100136.
20 (*a*) R. V. Slone, D. I. Yoon, R. M. Calhoun and J. T. Hupp, *J. Am. Chem. Soc.*, 1995, **117**, 11813–11814; (*b*) B. Manimaran, T. Rajendran, Y.-L. Lu, G.-H. Lee, S.-M. Peng and K.-L. Lu, *J. Chem. Soc., Dalton Trans.*, 2001, 515–517.
21 (*a*) T. C. Cheung, K. K. Cheung, S.-M. Peng and C.-M. Che, *J. Chem. Soc., Dalton Trans.*, 1996, 1645–1651; (*b*) W. Sun, H. Zhu and P. M. Barron, *Chem. Mater.*, 2006, **18**, 2602–2610.
22 I. Mathew, Y. Li, Z. Li and W. Sun, *Dalton Trans.*, 2010, **39**, 11201–11209.
23 J. Freudenreich, J. Furrer, G. Süss-Fink and B. Therrien, *Organometallics*, 2011, **30**, 942–951.
24 K.-I. Yamashita, K.-I. Sato, M. Kawano and M. Fujita, *New J. Chem.*, 2009, **33**, 264–270.
25 (*a*) B. Therrien and T. R. Ward, *Angew. Chem., Int. Ed.*, 1999, **38**, 405–408; (*b*) L. Mimassi, C. Cordier, C. Guyard-Duhayon, B. E. Mann and H. Amouri, *Organometallics*, 2007, **26**, 860–864; (*c*) H. Amouri and M. Gruselle, *Chirality in Transition Metal Chemistry: Molecules Supramolecular Assemblies and Materials*, John Wiley & Sons, Ltd, Chichester, 2009, pp. 121–177.
26 *HyperChem Computational Chemistry Software Package Version 7.5*, Hypercube Inc, Gainesville, Florida, 2003.
27 M. A. Galindo, M. Quirós, M. A. Romero and J. A. R. Navarro, *J. Inorg. Biochem.*, 2008, **102**, 1025–1032.
28 A. Bencini and V. Lippolis, *Coord. Chem. Rev.*, 2010, **254**, 2096–2180.
29 (*a*) O. Zava, J. Mattsson, B. Therrien and P. J. Dyson, *Chem.–Eur. J.*, 2010, **16**, 1428–143; (*b*) M. Groessl, Y. O. Tsybin, C. G. Hartinger, B. K. Keppler and P. J. Dyson, *JBIC, J. Biol. Inorg. Chem.*, 2010, **15**, 677–688; (*c*) P. Govender, N. C. Antonels, J. Mattsson, A. K. Renfrew, P. J. Dyson, J. R. Moss, B. Therrien and G. S. Smith, *J. Organomet. Chem.*, 2009, **694**, 3470–3476; (*d*) A. F. A. Peacock and P. J. Sadler, *Chem.–Asian J.*, 2008, **3**, 1890–1899; (*e*) S. H. van Riijt, H. Kostrhunova, V. Brabec and P. J. Sadler, *Bioconjugate Chem.*, 2011, **22**, 218–226.
30 (*a*) G. I. Pascu, A. C. G. Hotze, C. Sanchez-Cano, B. M. Kariuki and M. J. Hannon, *Angew. Chem., Int. Ed.*, 2007, **46**, 4374–4378; (*b*) A. Ghosh, P. Das, M. R. Gill, P. Kar, M. G. Walker, J. A. Thomas and A. Das, *Chem.–Eur. J.*, 2011, **17**, 2089–2098; (*c*) P. Govender, A. K. Renfrew, C. M. Clavel, P. J. Dyson, B. Therrien and G. S. Smith, *Dalton Trans.*, 2011, **40**, 1158–1167.
31 A. L. Harris, X. Yang, A. Hegmans, L. Povirk, J. J. Ryan, L. Kelland and N. P. Farrell, *Inorg. Chem.*, 2005, **44**, 9598–9600.
32 (*a*) F. Wang, J. Bella, J. A. Parkinson and P. J. Sadler, *JBIC, J. Biol. Inorg. Chem.*, 2005, **10**, 147–155; (*b*) O. Novakova, J. Kasparkova, V. Bursova, C. Hofr, M. Vojtiskova, H. Chen, P. J. Sadler and V. Brabec, *Chem. Biol.*, 2005, **12**, 121–129.
33 M. A. Bennett, T.-N. Huang, T. W. Matheson and A. K. Smith, *Inorg. Synth.*, 1982, **21**, 74–76.
34 F. Kühlwein, K. Polborn and W. Beck, *Z. Anorg. Allg. Chem.*, 1997, **623**, 1931–1944.